STUDY ON THE BEAM DYNAMICS IN THE RISP DRIVER LINAC

H.J. Kim, H.J. Jang, D. Jeon, IBS, Dajeon, Korea
J.-G. Hwang, E.S. Kim, KNU, Daegu, Korea

Abstract

Rare Isotope Science Project (RISP) has been proposed as a multi-purpose accelerator facility for providing beams of exotic rare isotopes of various energies. The RISP driver linac which is used to accelerate the beam, for an example, Uranium ions from 0.5 MeV/u to 200 MeV/u consists of superconducting RF cavities and warm quadrupole magnets for focusing heavy ion beams. Requirement of the linac design is especially high for acceleration of multiple charge beams. In this paper, we present the requirements of dynamic errors and correction schemes to minimize the beam centroid oscillation and preserve beam losses under control.

INTRODUCTION

The RISP (Rare Isotope Science Project) accelerator has been planned to study heavy ion of nuclear, material and medical science at the Institute for Basic Science (IBS). It can deliver ions from proton to Uranium with a final beam energy, for an example, 200 MeV/u for Uranium and 600 MeV for proton, and with a beam current range from 8.3 pμA (Uranium) to 660 pμA (proton) [1, 2]. The facility consists of three superconducting linacs of which superconducting cavities are independently phased and operating at three different frequencies, namely 81.25, 162.5 and 325 MHz.

The layout of the RISP accelerator is shown in Fig. 1. The Uranium ions produced in an electron cyclotron resonance ion source are preaccelerated to an energy of 500 keV/u by a radio frequency quadrupole and transported to the superconducting cavities by a medium energy beam transport. The driver linac is divided into three different sections: low energy superconducting linac (SCL1), charge stripper section and high energy superconducting linac (SCL2). Figure 2 shows a conceptual structure of SCL1 and SCL2. The SCL1 uses the two different families of superconducting resonators, i.e., quarter wave resonator (QWR) and half wave resonator (HWR). The SCL11 consists of 22 QWR's whose geometrical β is 0.047 and 22 doublets. The resonance frequency of QWR is 81.25 MHz. The cryomodule of the SCL11 hosts one superconducting cavity. The SCL12 consists of 123 HWR's whose geometrical β is 0.12 and 27 doublets. The resonance frequency of HWR is 162.5 MHz. This segment has the two families of cryomodules: one type of cryomodule hosts three superconducting cavities and the other hosts six superconducting cavities.

The SCL2 consists of the SCL21 and the SCL22, each consisting of geometric β 0.30, resonance frequency 325 MHz Single Spoke Resonators (SSR) and geometric β 0.53, resonance frequency 325 MHz SSR. Single Spoke Resonator type is chosen mainly because it can have a larger bore radius compared with the Half Wave Resonator type, which is very essential to reduce the uncontrolled beam loss in the high energy linac section. The number of cavities in the SCL21 and SCL22 is 84 and 144 respectively. The cryomodule of the SCL21 and SCL22 hosts 4 and 8 cavities respectively.Table 1 summarizes the parameter of four different superconducting cavities. The charge stripper section is located between SCL1 and SCL2. The charge stripper strips electrons from heavy ion beams to enhance the acceleration efficiency in the high energy linac section. The charge stripping section consists of four normal conducting quadrupole triplets and two room-temperature 45 degree bending magnets. The quadrupole

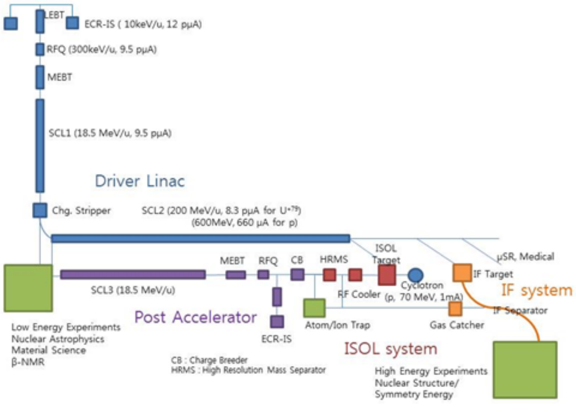

Figure 1: Layout of the RISP accelerator.

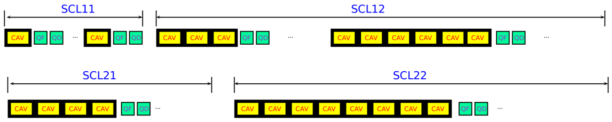

Figure 2: Layout of the SCL: SCL1 (top) and SCL2 (bottom).

Table 1: Superconducting Cavity Parameters

Parameter	Unit	QWR	HWR	SSR1	SSR2
Frequency	MHz	81.25	162.5	325	325
β_g		0.047	0.12	0.30	0.53
$L_{eff} = \beta_g \lambda$	m	0.173	0.221	0.277	0.470
Q	10^9	2.1	5	8	10
QR_s	Ω	21	50	80	108
R/Q	Ω	468	314	248	304
E_{acc}	MV/m	5.2	5.0	6.1	7.5
E_{peak}/E_{acc}		5.8	6.0	4.9	4.2
B_{peak}/E_{acc}	mT/(MV/m)	9.8	7.6	6.6	8.6

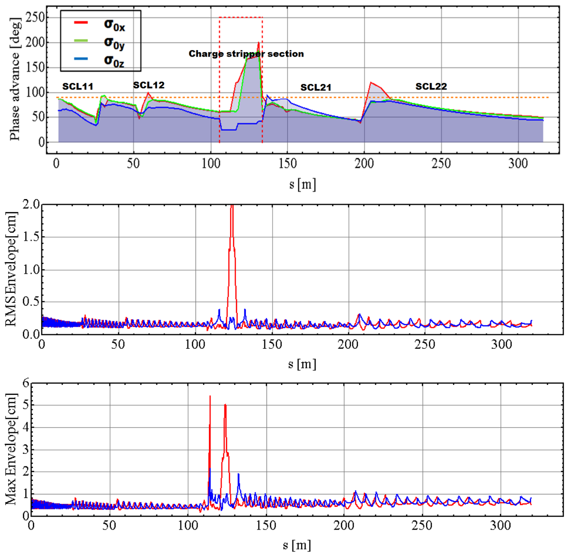

Figure 3: Phase advance per unit length (bottom) and maximum horizontal beam size envelope along the driver linac (top) without machine imperfections.

magnets provide adequate transverse focusing and beam matching to the SCL2 and bending magnet provides the momentum dispersion for the charge selection.

BEAM DYNAMICS SIMULATIONS

The RISP linac is a flexible structure to deliver heavy ions from proton to Uranium. The linac lattice is optimized by minimizing emittance growth and potential for beam loss by keeping a beam envelope smooth and regular. A transverse phase advance per period is kept under 90 degrees to prevent envelope instabilities. The ratio of transverse to longitudinal phase advance is kept in the range of 1.2 to 1.6 to avoid a resonance due to parametric coupling between longitudinal and transverse planes. Figure 3 shows phase advance per unit length along the length of the driver linac. The aperture radii of the low energy linac and the high energy linac are 40 mm and 50 mm respectively. At the charge stripper section, the aperture radius is around 100 mm. The maximum beam envelopes shown in Fig. 3 are kept less than 13 mm along the linac. Figure 4 shows an initial distribution of the particle at the entrance of driver linac. The initial particle coordinates of macro-particles are obtained by the particle tracking through the RFQ (radio frequency quadrupole). The initial charge state of uranium beam is 33 and 34. At the charge stripper section, the charge state are increased to 79 in average. The final distribution of the particle at the exit of driver linac is shown in Fig. 4. The color code represents the five charge states of uranium from 77 to 81. In the simulation, initial transverse emittance is 0.112 mm-mrad and 0.135 mm-mrad in x and y planes respectively. After passing through the charge stripper, the emittance increases. At the end of the driver linac, the emittance becomes 0.14 mm-mrad and 0.209 mm-mrad, as shown in Fig. 5. The longitudinal emittance is varied from 0.265 keV/u-ns to 5.51 keV/u-ns. The particle tracking with machine errors is performed with the TRACK code which has been developed in ANL [3].

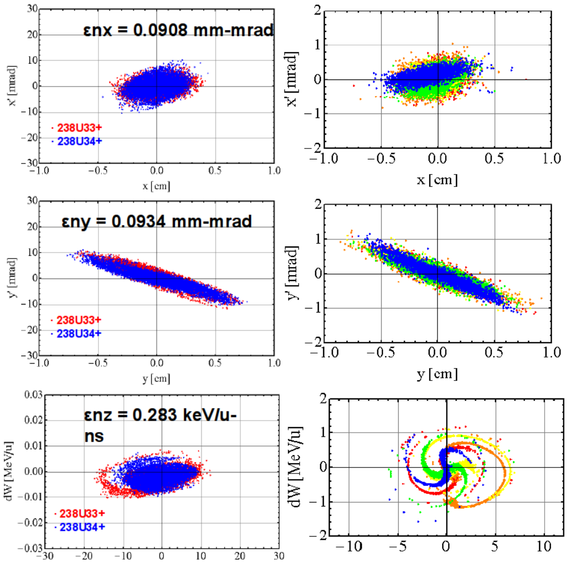

Figure 4: (left) Plot of initial distribution of the particle at the entrance of driver linac. (right) Plot of final distribution of the particle at the exit of driver linac. The color code represents the five charge states of uranium from 77 to 81.

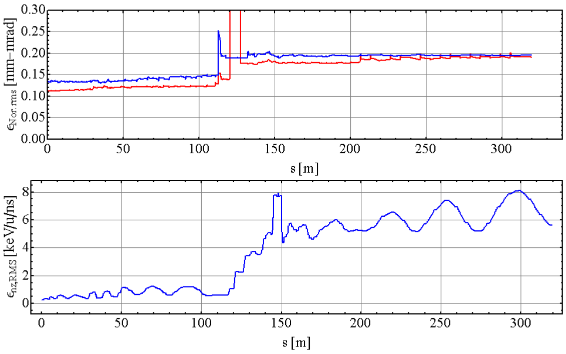

Figure 5: Plot of the transverse and longitudinal emittance variation in the driver linac.

For the actual SCL, machine imperfections cannot be avoided. The error comes from the misalignment of the linac elements and the limitation of manufacturing accuracy and various control errors. For instance, steering magnets are used to correct beam orbit displacements. In the baseline design of the RISP linac, steering magnets are placed where normal conducting quadrupoles are. The misalignment analysis includes all superconducting cavities and focusing elements assuming a uniform distribution. Table 2 summarizes tolerances for the lattice consisting of superconducting cavity and normal conducting quadrupole. It has been well known that the normal conducting quadrupole can be aligned in an accuracy of ±150 μm. The rotation angle about the z-axis is set to 5 mrad.

Table 2: Machine Imperfection of RISP Lattice Using Quadrupole as a Focusing Element. Displacement and rotation errors are uniformly generated. Phase and amplitude errors are 3 σ Gaussian.

Parameters	SC Cavity	Quadrupole
Displacement (mm)	±1	±0.15
Phase (deg)	±1	—
Amplitude (%)	±1	—
Rotation (mrad)	±5	±5

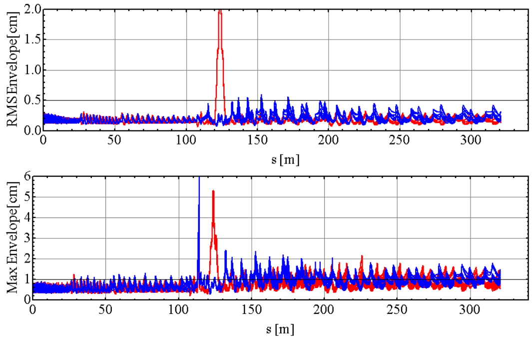

Figure 6: Plot of rms and maximum horizontal envelope for the driver linac due to machine imperfections.

The rotation angle is important due to the skew quadrupole term while it is independent of the solenoid due to symmetry of solenoid field. In the misalignment and RF error analysis, charge states of 33+ and 34+ of Uranium beams are used. Effect of machine imperfection on beam envelope is shown in Fig. 6. The maximum envelope is kept well below the transverse aperture 20 mm in the low energy linac. The envelope is under 25 mm in the high energy linac.

The post accelerator (SCL3) is designed to accelerate the rare isotopes produced in the ISOL (Isotope Separation On-Line) system. The SCL3 is, in principle, a duplicate of the driver linac up to low energy linear accelerator. The accelerated rare isotope beams are reaccelerated in the SCL2. Hence, the RISP accelerator provides a large number of rare isotopes with high intensity and with various beam energies. Between the SCL3 and SCL2, the charge stripper is installed. In case of Sn-132, the ECR provides $_{132}Sn^{+20}$. The charge state is increased to 45+ through the stripper. The 0.3 MeV/u beam at the entrance of SCL3 is accelerated up to 210 MeV/u at the end of SCL2. The transport line has four 45° bending magnets and three buncher cavities as shown in Fig. 7. The HWR cavity is used as the buncher. The optics at the transport line between SCL3 and SCL2 is shown in Fig. 8. The result of multi-particle tracking in the post-accelerator shows no uncontrolled beam loss in the transport line.

SUMMARY

Beam dynamics design of the RISP low and high energy linac in both the driver linac and the post-accelerator has been presented. In the design, the focusing in the superconducting linacs is provided by normal conducting quadrupole doublets. Four different cavities, such as QWR, HWR, SSR 1 and SSR 2, are used to accelerate the beam in the linac. We emphasize the stability of operation, flexibility of maintenance, and the minimization of beam loss. The linac design with normal conducting quadrupole gives a good beam quality.

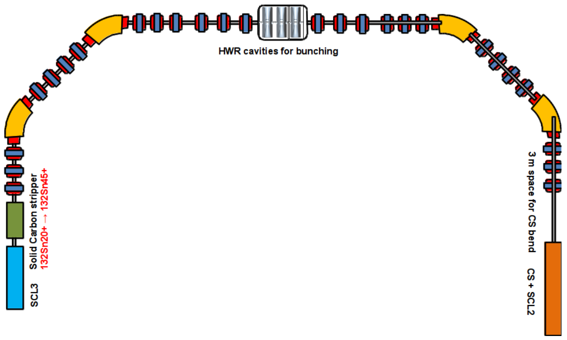

Figure 7: Layout of the transport line between SCL2 and SCL3 at the post-accelerator.

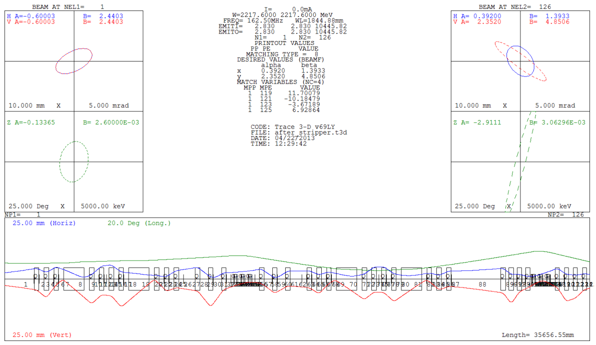

Figure 8: Plot of beam optics at the transport line between SCL3 and SCL2.

ACKNOWLEDGMENTS

This work was supported by the Rare Isotope Science Project which is funded by the Ministry of Science, ICT and Future Planning (MSIP) and the National Research Foundation (NRF) of the Republic of Korea under Contract 2011-0032011.

REFERENCES

[1] S.K. Kim et al, “Rare Isotope Science Project: Baseline Design Summary”, http://www.risp.re.kr/.

[2] D. Jeon et al, “Status of the RAON accelerator systems”, this conference.

[3] V.N. Aseev et al, Proceedings of 2005 Particle Accelerator Conference, Knoxville, Tennessee, p. 2053.